As–Sb exchange energies in tetrahedrite–tennantite fahlores and bournonite–seligmannite solid solutions

RICHARD O. SACK AND DENTON S. EBEL

Department of Earth and Atmospheric Sciences, Purdue University, West Lafayette, Indiana, 47907, U.S.A.

Abstract

Reversed brackets on As and Sb partitioning between tetrahedrite–tennantite fahlores $\{\sim Cu_{10}(Fe,Zn)_2(Sb,As)_4S_{13}\}$ and bournonite–seligmannite solid solutions $\{CuPb(Sb,As)S_3\}$ (400 °C, evacuated silica tubes, NH_4Cl flux) indicate that the maximum nonidealities associated with the As–Sb substitution are about 165 (bournonite) and 250 (fahlore) cal/gfw on a per atom exchange basis. The experimental constraints are consistent with the following calibration of the As–Sb exchange reaction between these phases:

$$RT\ln\left[\frac{(1-X_3^{FAH})\,X_{As}^{BRN}}{X_3^{FAH}\,X_{Sb}^{BRN}}\right]=\Delta\bar{G}^{o\,FB}_{As(Sb)_{-1}}+\frac{1}{4}\left(\Delta\bar{G}^{o}_{23}\,(X_2)+W^{FAH}_{AsSb}\,(1-2X_3)\right)-W^{BRN}_{AsSb}\,(1-2X^{BRN}_{As})$$

where $\Delta\bar{G}^{o\,FB}_{As(Sb)_{-1}}$ $\{\sim\Delta\bar{H}^{o}_{As(Sb)_{-1}}\} = -1.39 \pm 0.10$, $W^{FAH}_{AsSb} = 4.00 \pm 0.80$, and $W^{BRN}_{AsSb} = 0.66 \pm 0.18$ kcal/gfw, $X_2 \equiv Zn/(Zn + Fe)$ (or one-half the number of Zn atoms/formula unit) and $X_3 \equiv As/(As + Sb)$ refer to atomic ratios in fahlore, and $\Delta\bar{G}^{o}_{23} = \Delta\bar{H}^{o}_{23} = 2.59 \pm 0.14$ kcal/gfw (Raabe and Sack, 1984; Sack and Loucks, 1975; O'Leary and Sack, 1987; Sack, 1992).

KEYWORDS: fahlore, thermodynamics, bournonite, tetrahedrite, experiment, As–Sb–Cu–Pb–Fe–Zn–S, sulphosalt, geothermometer.

Introduction

THE fahlore mineral group (e.g. Ramdohr, 1969) exhibits the most extensive solid solution and widespread occurrence of all sulphosalts (cf. Takeuchi and Sadanaga, 1969). Tetrahedrite–tennantite is the most common mineral of the group, approximating $(Cu,Ag)_{10}(Fe,Zn)_2(Sb,As)_4S_{13}$ (tetrahedrite: Sb_4; tennantite, As_4) with trace Mn, Cd, and Hg for Fe and Zn, and Bi for As and Sb (e.g. Springer, 1969; Charlat and Levy, 1974; Pattrick, 1978). It is a principal source of mineable silver, commonly occurring in epithermal–mesothermal polymetallic base metal sulphide deposits of fissure-vein type. Fahlores in such veins are typically zoned in Ag–Cu, Zn–Fe, and As–Sb ratios in both time and space, with the most Cu-, As-rich and Ag-, Sb-poor fahlores deposited proximal to the hydrothermal source of the mineralising fluids, and with Ag and Sb exhibiting enrichment along outward flows paths (e.g. Goodell and Petersen, 1974; Wu and Petersen, 1977; Hackbarth and Petersen, 1984). These striking positive correlations between Sb/(Sb + As) and Ag/(Ag + Cu) ratios reflect (1) As–Sb fractionation between hydrothermal fluids and fahlores, (2) coupling of the energies of element substitutions induced by incompatibilities between As and Ag, Zn and Ag, and Zn and As in the fahlore structure, and (3) nonidealities in the substitutions of Ag for Cu and As for Sb in fahlore (Sack, 1992). Values for the energies of the reciprocal reactions defining these incompatibilities, and for the energetic effects associated with the Ag for Cu and Zn for Fe exchange substitutions, have been established from constraints on exchange reactions between fahlores and assemblages consisting of simpler sulphosalts, sulphides, and alloys (cf. Raabe and Sack, 1984; Sack and Loucks, 1985; O'Leary and Sack, 1987; Sack *et al.*, 1987; Ebel and Sack, 1989, 1991).

In this paper, we present results from As–Sb exchange experiments between tetrahedrite–ten-

Mineralogical Magazine, December 1993, Vol. 57, pp. 635–642

nantite fahlores and bournonite–seligmannite solid solutions. These experimental results are used to constrain the nonideality associated with the As–Sb substitutions in these minerals, and complete the calibration of a model for the thermodynamic mixing properties of tetrahedrite–tennantite (Sack *et al.*, 1987). Model miscibility gaps and the calibration for the As–Sb exchange reaction are compared with constraints from nature.

Experimental methods

Fahlores were synthesised as reported in Ebel and Sack (1989). Batches (4 gm) of bournonite–seligmannite solid solutions, $CuPbAs_xSb_{(1-x)}S_3$ with x = 0.0 (BN5), 0.2 (BN1), 0.4 (BN2), 0.6 (BN3), and 0.8 (BN4), were synthesised from simple sulphides in evacuated silica tubes with NH_4Cl flux. Synthesis reactions proceeded at temperatures near 400 °C for three month periods with regrinding (under alcohol), until homogeneity was evident from repetitive, random microprobe analysis. In a- and c-series experiments several large grains of one mineral were immersed in a large volume of the other minerals, to produce either fahlore-dominated or bournonite-dominated bulk compositions. In bournonite-dominated experiments (exps. a10–19, a30–59, and all of c-series experiments) several grains of medium to coarse-grained fahlore were combined with powdered bournonite (BN1, BN2, BN3, or BN4) such that the latter contained at least 90 mole percent of the semi-metals in the charge. The opposite procedure was employed in fahlore-dominated experiments (exps. a1–9 and a21–27). In d-series experiments in the Fe-free subsystem fahlore grains were immersed in a powdered bournonite : ZnS mixture (~1 : 9 mass ratio). Similar (unreported) experiments in the Zn-free subsystem were attempted using a 30 : 30 : 40 molar mixture of chalcopyrite : pyrite : FeS. Reactants were sealed in evacuated silica tubes with a small amount of NH_4Cl (<0.003 g), heated at 400 °C for several months (Table 1), and drop-quenched in water.

Experimental products were mounted in epoxy, polished, and analysed with the fully automated CAMECA SX-50 microprobe in the Department of Earth and Atmospheric Sciences of Purdue University. Standard operating conditions (15 kV, 20 nA cup current, 1 μm beam) were employed and the intensity data were reduced using the PAP correction scheme supplied by Cameca. Synthetic fahlores B32 = $Cu_{10}Fe_2As_4S_{13}$ (Fe, $K\alpha$; As, $K\alpha$), B41 = $Cu_{10}Zn_2Sb_4S_{13}$ (Sb, $L\alpha$), and B42 = $Cu_{10}Zn_2As_4S_{13}$ (Cu, $K\alpha$; Zn, $K\alpha$; S, $K\alpha$) (Ebel and Sack, 1989) were used as standards (elements, emission lines) for the product fahlores of bournonite-dominated experiments. Fahlores were found to be 'lead-free' in all cases. Standards for all other analyses reported in Table 1 were as follows: BN2 = $CuPbAs_{0.4}Sb_{0.6}S_3$ (Cu, $K\alpha$; Pb, $M\alpha$; S, $K\alpha$), BN4 = $CuPbAs_{0.8}Sb_{0.2}S_3$ (As, $L\alpha$), BN5 = $CuPbSbS_3$ (Sb, $L\alpha$), B32 (Fe, $K\alpha$), and B42 (Zn, $K\alpha$).

Experimental results

In Table 1 microprobe analyses for fahlores and bournonites that exhibit the greatest detected changes in As/(As + Sb) ratio during exchange experiments are presented. Also presented are representative analyses of other run products. Despite protracted run durations (Table 1), the experiments did not produce pervasive As–Sb exchange in either fahlore or bournonite solutions. In each bournonite-dominated experiment, fahlore exhibiting maximum deviation from nominal As/(As + Sb) ratio was confined to the outermost rims (<20 μm) of grains in immediate proximity to the bournonite medium. These products presumably resulted from recrystallisation or grain growth, as the overwhelming bulk of the grains exhibit negligible zoning or deviations from nominal As/(As + Sb) ratios. Changes in As/(As + Sb) were more difficult to detect in bournonites (from fahlore-dominated experiments) than in fahlores (from bournonite-dominated experiments). Such changes were readily detected only in d-series experiments in the Zn system where ZnS underwent extensive recrystallisation adjacent to contacts between fahlores and the bournonite medium.

In most bournonite-dominated a- and c-series experiments, despite the apparently sluggish kinetics of the As–Sb exchange reaction, the product fahlores exhibit noticeable and pervasive deviations from nominal $Cu_{10}(Fe,Zn)_2(Sb,As)_4S_{13}$ stoichiometry, approximating $Cu_{10+x}(Fe,Zn)_{2-x}(Sb,As)_4S_{13}$ (e.g. Sack and Loucks, 1985) with x between zero and about 0.6. The extent of operation of the Cu–Fe and Cu–Zn exchanges appears to be highly dependent on the Zn/(Zn + Fe) ratio (Fig. 1), with zinc fahlores typically exhibiting the least deviation from the nominal formula and values of x increasing with decreasing Zn/(Zn + Fe). In contrast, deviations from nominal stoichiometry were not evident in fahlores processed in fahlore-dominated experiments, nor in bournonite-dominated experiments (d-series) to which ZnS (or the chalcopyrite + pyrite + FeS assemblage) had been added to the

Table 1. Run conditions, initial As/(As+Sb) ratios, and final sulfosalt compositions (wt. %). Standard deviations (σ) for N analyses are indicated.

label*	phase	X_2^{FAH}	X_3^{FAH}	X_{As}^{BRN}	N	Cu	σ	Pb	σ	Fe	σ	Zn	σ	Sb	σ	As	σ	S	σ	sum
1a	brn	0.502	0.80	0.80	6	13.97	(0.23)	44.32	(0.23)					10.99	(0.16)	9.49	(0.50)	20.85	(0.09)	99.62
1c	fah	1.00	1.00	0.80	3	41.73	(0.37)					8.06	(0.07)	2.49	(0.12)	18.00	(0.48)	27.98	(0.63)	98.26
1d	fah	1.00	0.50	0.20	1	37.66						8.53		18.17		7.32		26.07		97.75
2c	fah	1.00	1.00	0.80	2	44.10	(0.27)					8.16	(0.07)	2.29	(0.04)	19.84	(0.58)	27.94	(0.18)	101.97
2c	brn	1.00	1.00	0.80	2	13.12	(0.38)	46.03	(0.23)					4.44	(0.37)	13.28	(0.07)	21.98	(0.22)	98.85
3c	sin	1.00	0.50	0.80	2	37.75	(0.17)					0.04	(0.03)	1.35	(0.09)	29.10	(0.40)	29.09	(0.40)	97.33
3d	fah	1.00	1.00	0.40	3	39.61	(0.15)					8.75	(0.10)	10.59	(0.14)	12.65	(0.44)	26.82	(0.19)	98.42
5a	brn	0.550	0.60	0.40	12	13.37	(0.27)	43.18	(0.63)					17.21	(0.43)	5.29	(0.19)	20.10	(0.21)	99.15
5d	fah	1.00	1.00	0.60	4	40.86	(0.33)					9.00	(0.30)	6.27	(0.15)	15.26	(0.19)	27.26	(0.35)	98.65
5d	brn	1.00	1.00	0.60	3	13.99	(0.11)	44.64	(0.12)					10.08	(0.16)	10.34	(0.10)	21.08	(0.10)	100.13
6a	brn	0.526	0.70	0.80	8	14.02	(0.24)	43.99	(0.69)					12.85	(0.14)	8.54	(0.20)	20.49	(0.28)	99.89
7a	brn	0.526	0.70	0.40	4	13.77	(0.09)	43.98	(0.54)					15.27	(0.21)	6.73	(0.08)	20.25	(0.22)	100.00
7c	fah	0.00	0.50	0.80	4	43.81	(0.20)			6.23	(0.20)			2.14	(0.12)	19.23	(0.42)	19.23	(0.42)	99.22
7c	brn	0.00	0.50	0.80	2	14.03	(0.18)	46.44	(0.36)					5.47	(0.06)	13.01	(0.21)	21.82	(0.13)	100.78
7c	pbs	0.00	0.50	0.80	2	1.32	(0.30)	42.34	(0.44)	0.11	(0.04)	0.02	(0.02)	15.81	(0.42)	17.62	(0.01)	24.42	(0.28)	101.64
9c	fah	1.00	0.50	0.20	2	42.22	(0.63)					6.41	(0.16)	16.72	(0.11)	8.82	(0.11)	26.21	(0.08)	100.38
9c	fam	1.00	0.50	0.20	4	47.18	(0.76)			0.04	(0.03)	0.09	(0.06)	10.35	(0.27)	11.92	(0.38)	30.88	(0.49)	100.46
11a	fah	0.00	1.00	0.40	2	42.49	(0.59)			5.94	(0.07)			8.06	(0.33)	15.02	(0.18)	26.35	(0.27)	97.86
11c	fah	1.00	0.00	0.20	5	39.21	(0.24)					6.61	(0.15)	19.88	(0.26)	6.12	(0.12)	25.61	(0.23)	97.43
11c	cst	1.00	0.00	0.20	1	24.81								47.04		0.91		25.28		98.04
12a	fah	0.00	0.50	0.40	4	41.98	(0.24)			5.63	(0.11)			9.95	(0.25)	13.51	(0.25)	26.48	(0.20)	97.55
12c	fah	1.00	1.00	0.20	3	40.37	(0.29)					7.25	(0.08)	14.90	(0.09)	10.45	(0.34)	26.46	(0.02)	99.43
12c	fam	1.00	1.00	0.20	8	46.92	(0.22)					0.02	(0.02)	3.14	(0.22)	16.92	(0.50)	32.04	(0.11)	99.04
13a	fah	0.00	0.50	0.40	6	41.84	(0.26)			6.19	(0.07)			10.21	(0.17)	13.09	(0.20)	26.88	(0.23)	98.21
13d	fah	1.00	1.00	0.80	6	41.79	(0.25)					9.00	(0.12)	2.46	(0.01)	18.15	(0.28)	27.67	(0.11)	99.07
13d	brn	1.00	1.00	0.80	2	14.20	(0.35)	45.81	(0.03)					5.25	(0.01)	13.66	(0.10)	21.70	(0.25)	100.62
14a	fah	0.550	0.60	0.40	4	40.77	(0.67)			3.21	(0.03)	4.17	(0.32)	10.82	(0.51)	25.52	(0.31)	26.52	(0.31)	97.94
14c	fah	0.00	1.00	0.20	4	41.90	(0.42)			5.13	(0.10)			14.64	(0.17)	10.16	(0.17)	26.37	(0.14)	98.20
14c	brn	0.00	1.00	0.20	7	13.33	(0.11)	42.86	(0.17)					20.19	(0.14)	3.65	(0.12)	20.19	(0.10)	100.22
15c	fah	1.00	1.00	0.40	2	42.80	(0.29)					7.52	(----)	10.38	(0.16)	13.60	(0.11)	27.01	(0.11)	101.31
16c	fah	1.00	1.00	0.40	2	42.40	(0.44)					7.66	(0.18)	10.05	(0.11)	13.30	(0.17)	26.88	(0.29)	100.29
17a	fah	1.00	0.50	0.40	6	39.86	(0.23)					7.66	(0.12)	12.67	(0.17)	11.03	(0.18)	26.98	(0.25)	98.20
17c	fah	0.00	0.50	0.40	2	41.90	(0.36)			5.96	(0.11)			10.60	(0.11)	13.06	(0.31)	26.98	(0.11)	98.50
17c	brn	0.00	0.50	0.40	1	13.17		43.98						16.26		6.15		20.71		100.27
19a	fah	1.00	0.00	0.40	4	38.88	(0.36)					7.99	(0.08)	18.63	(0.55)	7.56	(0.11)	25.64	(0.22)	98.70
23a	pbs	1.00	0.50	0.00	2	0.58	(0.03)	45.21	(0.03)			0.07	(0.02)	27.42	(0.25)	4.59	(0.09)	19.85	(0.07)	97.72
24a	fah	0.00	0.50	0.00	1	40.56				7.58				16.02		10.11		26.91		101.18
24a	pbs	0.00	0.50	0.00	4	0.40	(0.15)	60.20	(0.35)	0.05	(0.04)			19.89	(0.20)	1.06	(0.03)	15.83	(0.17)	97.43
24a	cpy	0.00	0.50	0.00	2	33.23	(0.52)			32.28	(0.65)			0.03	(0.02)	0.06	(----)	34.21	(0.31)	99.81
25a	fah	0.00	0.50	0.2	2	39.73	(0.43)			7.31	(0.01)			12.09	(0.01)	12.29	(0.09)	26.86	(0.13)	98.28
25a	pbs	0.00	0.50	0.2	1	0.15		61.41		0.09				18.81		1.66		15.50		97.62
25a	cpy	0.00	0.50	0.2	1	33.15				33.06						0.03		34.41		100.65
26c	fah	0.00	0.50	0.60	1	44.94				6.45				4.65		17.71		28.00		101.75
37a	fah	1.00	0.00	0.40	4	38.20	(0.52)					7.67	(0.12)	24.42	(0.77)	3.22	(0.42)	25.28	(0.30)	98.79
41a	fah	1.00	0.00	0.20	3	40.56	(0.16)			5.56	(0.06)			20.15	(0.11)	6.46	(0.07)	26.36	(0.10)	99.09
42a	fah	0.00	0.50	0.20	9	41.03	(0.41)			6.20	(0.12)			15.51	(0.70)	9.67	(0.45)	25.80	(0.40)	98.21
50a	fah	1.00	0.00	0.60	4	40.90	(0.17)					7.64	(0.07)	7.42	(0.11)	15.28	(0.48)	26.83	(0.11)	98.07
53a	fah	1.00	1.00	0.60	4	41.92	(0.13)					8.26	(0.19)	5.67	(0.02)	16.60	(0.20)	27.42	(0.07)	99.87
54a	fah	1.00	0.50	0.60	6	40.84	(0.26)					7.94	(0.17)	8.32	(0.32)	14.46	(0.14)	26.99	(0.14)	98.55
56a	fah	0.00	0.00	0.60	7	41.50	(0.51)			6.87	(0.14)			6.59	(0.15)	16.15	(0.42)	27.27	(0.34)	99.38
59a	fah	0.00	1.00	0.60	7	43.33	(0.18)			6.13	(0.12)			4.26	(0.30)	17.37	(0.38)	27.80	(0.23)	98.89
J–c#	fah				13	29.52	(0.60)			0.57	(0.17)	6.59	(0.30)	22.11	(0.67)	3.28	(0.44)	24.35	(0.30)	98.27
J–c#	brn				8	12.96	(0.27)	42.72	(0.70)					19.53	(0.75)	3.01	(0.48)	20.35	(0.25)	98.87

* Run times for a–, c–, d–series experiments were 2802, 2784, and 5351 hours, respectively. Phase abbreviations are as follows: fah, fahlore, brn, bournonite–seligmannite; cst, chalcostibite; sin, sinnerite; fam, famatinite–luzonite solid solution; cpy, chalcopyrite; pbs, miscellaneous lead sulfosalts.

Fahlore from area c in Julcani sample 8764 (J–c) contains 11.42(0.69) wt. % Ag, 0.22(0.16) wt.% Hg, and 0.17(0.15) wt. % Bi ; bournonite contains 0.01(0.03) wt. % Ag and 0.29(0.16) wt.% Hg.

bournonite medium. In extreme cases loss of Fe or Zn from fahlores led to the formation of secondary Fe- and Zn-poor sulphosalts, including chalcostibite, sinnerite, and famatinite (e.g. Luce *et al.*, 1977). In some Fe-bearing experiments, either (1) fahlore-dominated with Sb/(As + Sb) of fahlore >0.6 and no buffer assemblage or (2) bournonite-dominated with Sb/(As + Sb) of bournonite = 0.8 and a cpy:pyr:FeS buffer assemblage, the fahlore and bournonite reacted to produce various Pb and Cu sulphosalts (e.g. boulangerite, phase II of Craig *et al.*, 1973) and chalcopyrite.

Thermodynamics

In principle, the energetic consequences of the As–Sb substitutions in fahlore and bournonite–seligmannite can be evaluated from the experimental brackets on their exchange isotherms.

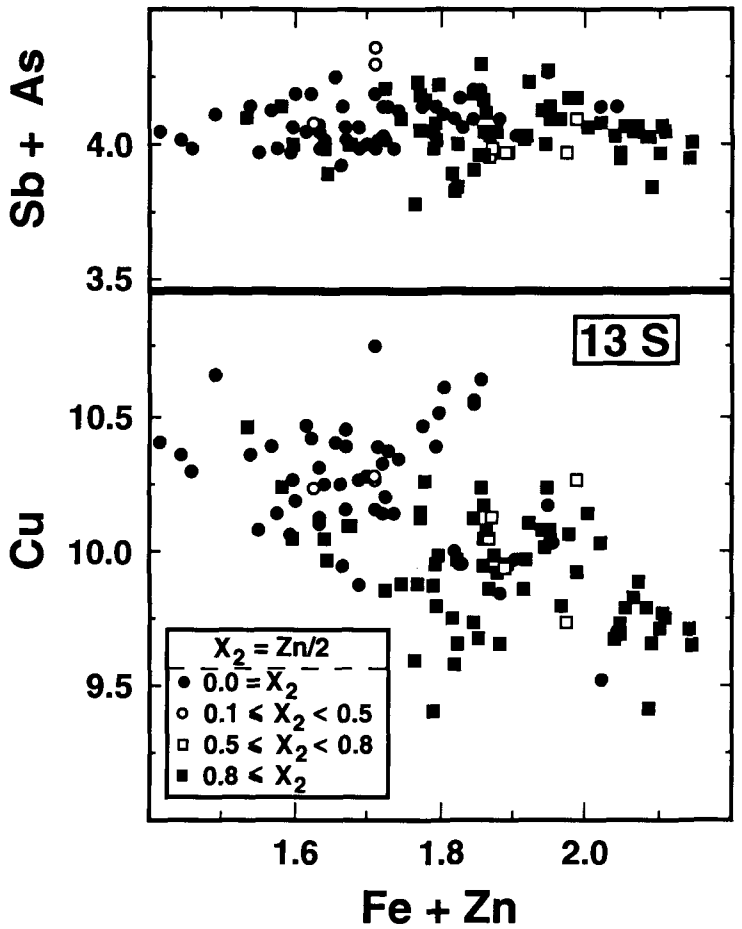

FIG. 1. Atoms of Cu, (Fe + Zn), and (Sb + As) in experimental tetrahedrite–tennantite fahlores expressed on a 13 sulphur formula unit basis. Solid circles and squares represent zinc- and iron-free fahlores, open circles indicate natural silver-poor, iron-rich tetrahedrite–tennantites which coexist with bournonite–seligmannites from the Rajpura–Dariba polymetallic deposit (Mishra and Mookerjee, 1986), and open squares represent both synthetics with intermediate Zn/(Zn + Fe) ratios and a zincian tetrahedrite–tennantite from Rajpura–Dariba (lowest Cu).

$Cu_{10}(Fe,Zn)_2(Sb,As)_4S_{13}$ fahlores are reciprocal solutions in which As and Zn are incompatible. This incompatibility between As and Zn is expressed by a positive Gibbs energy of the reciprocal reaction

$$Cu_{10}Zn_2Sb_4S_{13} + Cu_{10}Fe_2As_4S_{13} = Cu_{10}Fe_2Sb_4S_{13} + Cu_{10}Zn_2As_4S_{13} \quad (1)$$

($\Delta\bar{G}^{o}_{23} = 2.59 \pm 0.14$ kcal/gfw; Raabe and Sack, 1984; Sack and Loucks, 1985; O'Leary and Sack, 1987). The incompatibility induces a splitting in the As–Sb exchange isotherms (Fig. 2) that is augmented by the nonideality associated with As–Sb substitution. Because the magnitude of the splitting due to this incompatibility is known, the nonideality associated with the As–Sb substitution can be determined from the magnitude of the observed splitting in the As–Sb exchange isotherms.

We may analyse the As–Sb exchange isotherms using the formulation of Sack *et al.* (1987) for the thermodynamic properties of $(Cu,Ag)_{10}(Fe,Zn)_2(Sb,As)_4S_{13}$ fahlores, given the assumptions of (1) strictly regular binary solution behaviour of bournonite–seligmannite and (2) negligible energetic consequences of deviations from the nominal stoichiometric formula of fahlore. For these approximations, we may write the following equation for the condition of As–Sb exchange equilibrium between these phases,

$$0 = (\partial\bar{G}^{BRN}/\partial X^{BRN}_{CuPbSbS_3}) + \frac{1}{4}(\partial\bar{G}^{FAH}/\partial X_{Cu_{10}Fe_2As_4S_{13}}), \text{ or:}$$

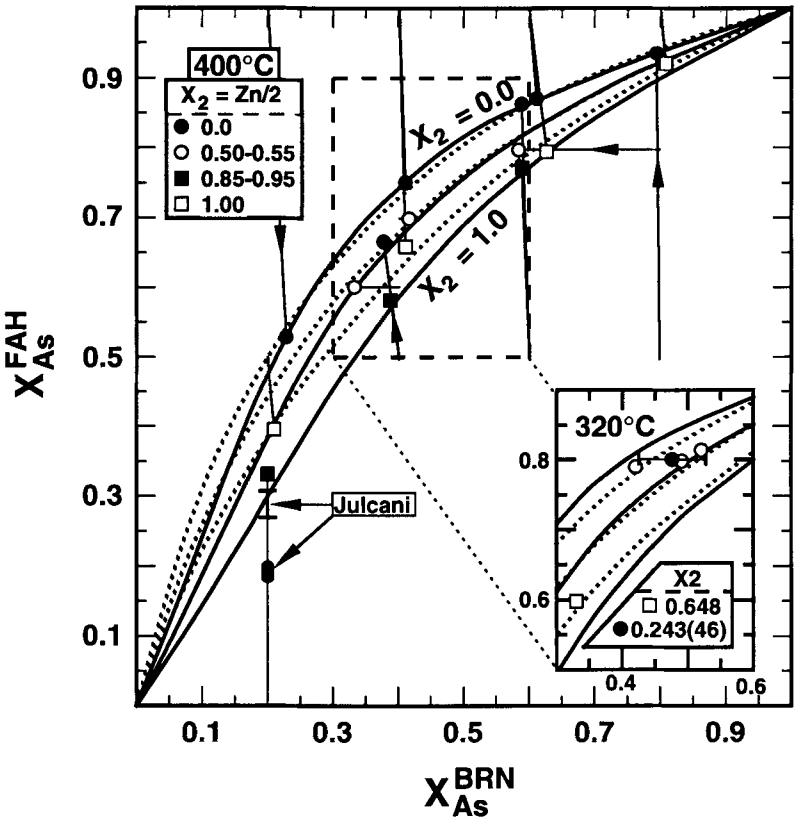

FIG. 2. Comparison of calculated 400 °C As–Sb distribution isotherms and As/(As + Sb) atomic ratios of product bournonites and fahlores. Symbols are coded according to X_2 in fahlores as follows: solid circles, zinc-free; open circles, $0.50 \leq X_2 \leq 0.55$; solid squares, $0.85 \leq X_2 \leq 0.95$ (line segment below, a- and c-series experiments), open squares, $X_2 \geq 1.0$ (line segment above, d-series experiments). As/(As + Sb) ratios are taken from Table 1 or are estimated from nominal compositions. Ends of line segments indicate nominal As/(As + Sb) ratios of fahlores and bournonites. Solid ellipse indicates one bournonite-argentian fahlore pair from Julcani (Table 1). Error bracket above the solid ellipse indicates the As/(As + Sb) ratios corresponding Ag-free fahlores would have at 200 (top bracket) and 400 °C (bottom bracket), according to the calibration of Ebel and Sack (1989, 1991). Curves indicate 400 °C As–Sb distribution isotherms (X_2 = 0.00, 0.50, and 1.00) calculated from eq. (2) for $\Delta\bar{G}^{o}_{23} = \Delta H^{o}_{23} = 2.59$ kcal/gfw, utilising $W^{FAH}_{AsSb} = 0.00$ kcal/gfw (dotted) and $W^{FAH}_{AsSb} = 4.00$ kcal/gfw (solid), and functional relationships $W^{BRN}_{AsSb}(W^{FAH}_{AsSb})$ and $\Delta\bar{G}^{oFB}_{As(Sb)-1}(W^{FAH}_{AsSb})$ permitted by the brackets on As–Sb partitioning between bournonites and Zn-free fahlores for these choices for W^{FAH}_{AsSb}:$W^{BRN}_{AsSb} = 0.00$ and $\Delta\bar{G}^{oFB}_{As(Sb)-1} = \Delta\bar{H}^{oFB}_{As(Sb)-1} = -1.8856$ for $W^{FAH}_{AsSb} = 0.00$ kcal/gfw, and $W^{BRN}_{AsSb} = 0.7222$ and $\Delta\bar{G}^{oFB}_{As(Sb)-1} = -1.3446$ for $W^{FAH}_{AsSb} = 4.00$ kcal gfw. Portions of the corresponding 320 °C curves appearing in insert are compared with the As/(As + Sb) ratios of coexisting fahlores and bournonites from the Rajpura-Dariba polymetallic deposit (Mishra and Mookerjee, 1986).

$$RT\ln\left[\frac{X^{FAH}_{Sb}\,X^{BRN}_{As}}{X^{FAH}_{As}\,X^{BRN}_{Sb}}\right] = \Delta\bar{G}^{oFB}_{As(Sb)-1} + \frac{1}{4}\left(\Delta\bar{G}^{o}_{23}(X_2) + W^{FAH}_{AsSb}(1-2X_3)\right) - W^{BRN}_{AsSb}(1-2X^{BRN}_{As}). \quad (2)$$

In this equation $\Delta\bar{G}^{oFB}_{As(Sb)-1}$ and $\Delta\bar{G}^{o}_{23}$ are the standard state Gibbs energies of the As–Sb exchange reaction

$$\frac{1}{4}Cu_{10}Fe_2Sb_4S_{13} + CuPbAsS_3 = \frac{1}{4}Cu_{10}Fe_2As_4S_{13} + CuPbSbS_3, \quad (3)$$

and reaction (1); W^{FAH}_{AsSb} and W^{BRN}_{AsSb} are the binary regular solution parameters describing deviations from linearity in the *vibrational* Gibbs energy

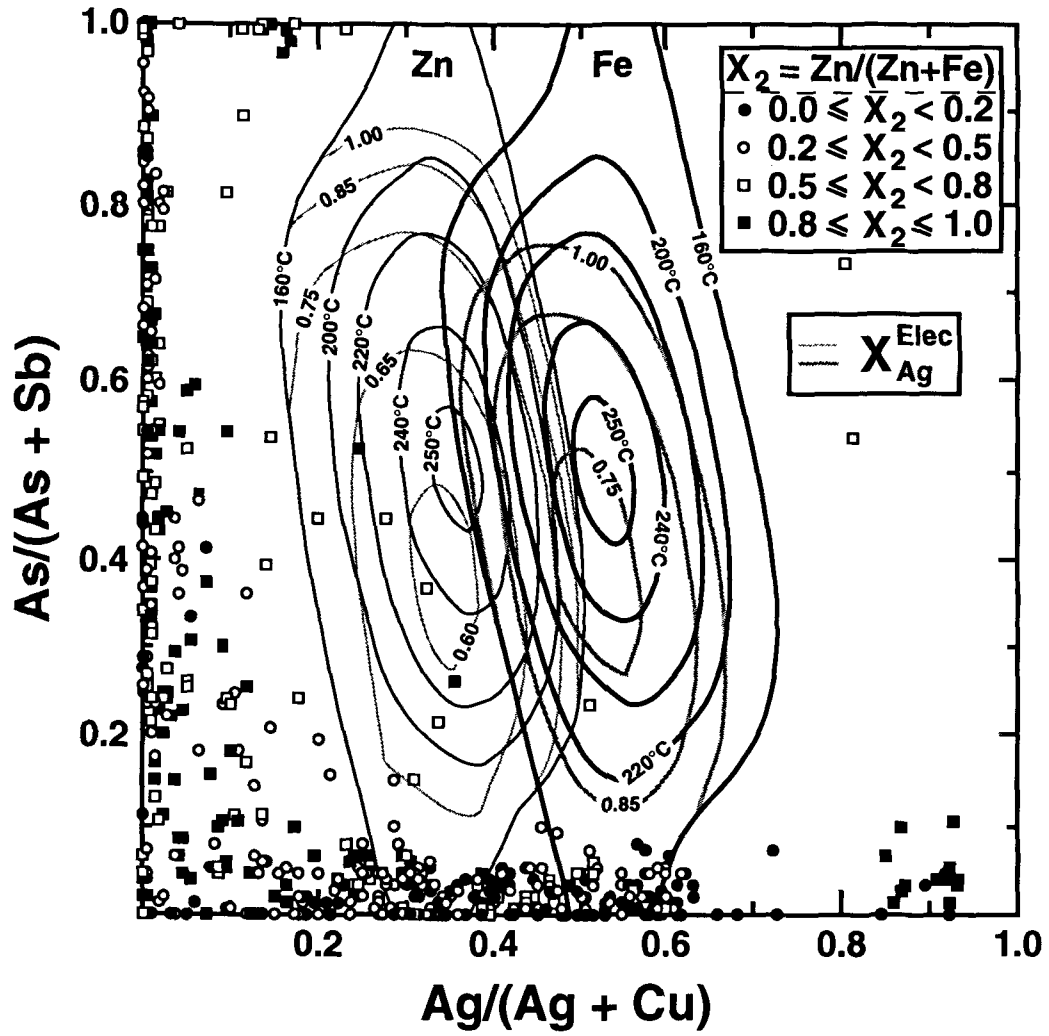

FIG. 3. Comparison of calculated 160, 200, 220, 240, and 250 °C miscibility gaps for $(Cu,Ag)_{10}Zn_2(Sb,As)_4S_{13}$ and $(Cu,Ag)_{10}Fe_2(Sb,As)_4S_{13}$ fahlores (solid curves) with reported natural compositions. The isotherms are overlain by contours of Ag/(Ag + Au) ratios of electrum (gold–silver alloy). The intersections of miscibility-gap isotherms with isopleths of electrum composition (X_{Ag}^{Elec} of 0.60, 0.65, 0.75, 0.85, and 1.00) define tielines for coexisting fahlores that are in Ag–Cu exchange equilibrium with these electrums, chalcopyrite, and pyrite according to the calibration of Ebel and Sack (1989, 1991). Sources of compositional data are referenced in Sack *et al.* (1987), Sack (1992), or are from Akande (1985), Charnock *et al.* (1989), Gemell *et al.* (1989), Kase (1988), Lynch (1989), Naik (1975), Pearson *et al.* (1988), Schmid *et al.* (1990), and Yigitgüden and Friedrich (1986).

along the fahlore joins $Cu_{10}Zn_2(As,Sb)_4S_{13}$ and $Cu_{10}Fe_2(As,Sb)_4S_{13}$, and in $CuPb(As,Sb)S_3$ solid solutions; $X_2 \equiv Zn/(Zn + Fe)$ and $X_3 \equiv As/(As + Sb) = X_{As}^{SM}/(X_{As}^{SM} + X_{Sb}^{SM})$ refer to atomic ratios in fahlore, and X_{As}^{BRN} is the ratio As/(As + Sb) in bournonite–seligmannite solid solution.*

SF * In neglecting the energetic consequences of deviations from the nominal, stoichiometric fahlore formula, we have implictly assumed that $X_2 = Zn/2$.

Interpreted in light of equation (2), the brackets on As–Sb partitioning between bournonites and Zn-free fahlores (Fig. 2) require the nonideality associated with the As–Sb substitution in fahlore to be less than about 300 cal/gfw per site ($W_{AsSb}^{FAH} < 4.8$ kcal/gfw), to satisfy relationships between the parameters W_{AsSb}^{FAH}, W_{AsSb}^{BRN}, and $\Delta\bar{G}^{oFB}_{As(Sb)_{-1}}$. The brackets tightly constrain W_{AsSb}^{BRN} and $\Delta\bar{G}^{oFB}_{As(Sb)_{-1}}$ as functions of

W^{FAH}_{AsSb} and, by themselves, they are consistent with the inference either that As and Sb mix ideally in fahlore and bournonite or that fahlores exhibit greater positive deviations from ideality of As–Sb mixing than do bournonites (cf. Fig. 2). These relationships, $W^{BRN}_{AsSb}(W^{FAH}_{AsSb})$ and $\Delta\bar{G}^{oFB}_{As(Sb)-1}$ (W^{FAH}_{AsSb}), also are broadly consistent with brackets obtained for fahlores with intermediate Zn/(Zn + Fe) ratios (fahlore-dominated experiments) only if $W^{FAH}_{AsSb} \leq 4.8$ kcal/gfw. Finally, a value of W^{FAH}_{AsSb} of 4.0 ± 0.8 kcal/gfw, satisfies all experimental brackets (Fig. 2) and produces maximal accord with petrological constraints discussed below. For this estimated W^{FAH}_{AsSb}, the following optimal values for the remaining two parameters in equation (2) are obtained: $\Delta\bar{G}^{oFB}_{As(Sb)-1} = -1.39 \pm 0.10$ and $W^{BRN}_{AsSb} = 0.66 \pm 0.18$ kcal/gfw.

As–Sb partitioning relations between fahlore and bournonite–seligmannite solid solutions in the Rajpura–Dariba polymetallic deposit, Poona, India (Mishra and Mookherjee, 1986) and the Julcani mining district, Peru (Goodell and Petersen, 1974) provide evidence that W^{FAH}_{AsSb} is near the upper boundary established from the experimental data, 4.8 kcal/gfw. Assuming that the entropy of the As–Sb exchange reaction (eq. 3) is zero (cf. Sack and Ghiorso, 1989), Mishra and Mookherjee's data are consistent with an equilibration temperature of about 320 °C, as deduced from our calibration of equation (2). The X_2 dependence of As/(As + Sb) ratios of coexisting Rajpura–Dariba bournonite–Ag-poor fahlore pairs is in accord with the experimentally derived value, $W^{FAH}_{AsSb} = 4.0 \pm 0.8$ kcal/gfw, but it is too pronounced to be reconciled with the proposition that As and Sb exhibit ideal mixing in fahlore and bournonite (cf. Fig. 2). A similar conclusion may be drawn from bournonite–argentian fahlore-bearing ores from the Julcani mining district, in which bournonites are intimately intergrown with Ag- and Zn-rich fahlores. Although most of the fahlore–bournonite pairs for which we obtained microprobe data are too Sb-rich to provide useful constraints, the most arsenian pair examined (Table 1) exhibits an As–Sb, fahlore–bournonite partition coefficient inconsistent with our calibration of the As–Sb exchange reaction, unless W^{FAH}_{AsSb} reaches to, or exceeds, the upper bound given above (Fig. 2).

It is noteworthy that the estimated equilibration temperature for the As–Sb exchange reaction between Ag-poor fahlores and bournonites (320 °C) is substantially higher than that obtained for coexisting sphalerites and argentian fahlores of the Rajpura–Dariba polymetallic deposit using the calibration of O'Leary and Sack (1987) for the Fe–Zn exchange reaction between these phases, 230 ± 35 °C (Ebel and Sack, 1989). If these estimated equilibration temperatures reflect retrograde cooling, then As–Sb exchange is more refractory than Fe–Zn exchange in fahlore, as we have observed experimentally. It is also noteworthy that miscibility gaps for Zn- and Fe-bearing argentian fahlores calculated using our estimate for the nonideality in the As–Sb substitution, and the thermodynamic model of Sack (1992), are in excellent agreement with the composition data for natural fahlores crystallised over the 200–350 °C temperature range (Fig. 3). Finally, 75 °C miscibility gaps in polybasite-pearceite solids solutions $[(Cu_x,Ag_{1-x})_{16}(As,Sb)_2S_{11}, 0.06 < x < 0.57]$ with intermediate Cu/(Cu + Ag) and As/(As + Sb) ratios require that the maximum nonideality associated with the As–Sb substitution in this phase is with the range found for bournonites and fahlores, ≥165 and ≤250 cal/gfw on a per atom exchange basis (Harlov and Sack, in prep.).

Acknowledgements

We thank W. Azeredo and C. Hager for technical assistance, P. C. Goodell for loaning samples from Julcani, and an anonomous referee for helpful comments. Material support was provided by the National Science Foundation through grant EAR89-04270.

References

Akande, S. O. (1985) Coexisting precious metals, sulfsalts and sulfide minerals in the Ross gold mine, Holtyre, Ontario. *Can. Miner.*, **23**, 95–8.

Charlat, M. and Levy. C. (1974) Substitutions multiples dans la serie tennantite-tetrahedrite. *Bull. Soc. Franc. Minéral. Cristallogr.*, **97**, 241–50.

Charnock, J. M., Garner, C. D., Pattrick, R. A. D., and Vaughan, D. J. (1989) EXAFS and Mössbauer spectroscopic study of Fe-bearing fahlores. *Mineral. Mag.*, **53**, 193–9.

Craig, J. R., Chang, L. L. Y., and Lees, W. R. (1973) Investigations in the PbSbS system. *Can. Mineral.*, **12**, 199–206.

Ebel, D. S. and Sack, R. O. (1989) Ag–Cu and As–Sb exchange energies in tetrahedrite–tennantite fahlores. *Geochim. Cosmochim. Acta*, **53**, 2301–9.

——— (1991) Arsenic–silver incompatibility in fahlore. *Mineral. Mag.*, **55**, 521–8.

Gemmell, J. B., Zantop, H., and Birnie, R. W. (1989 Silver sulfosalts of the Santo Niño vein, Fresnillo District, Zactecas, Mexico. *Can. Mineral.*, **27**, 401–8.

Goodell, P. C. and Petersen, U. (1974) Julcani mining district, Peru: A study of metal ratios. *Econ. Geol.*, **69**, 347–61.

Hackbarth, C. J. and Petersen, U. (1984) Systematic compositional variations in Argentian tetrahedrite. Ibid., **79**, 448–60.

Kase, K. (1988) Tin, arsenic, zinc and silver mineralisation in the Besshi mine, Central Shikoku, Japan. *Mining Geol.*, **38**, 407–18.

Luce, F. D., Tuttle, C. L., and Skinner, B. J. (1977) Studies of sulfosalts of copper. V. Phases and phase relations in the system Cu–Sb–As–S between 350 °C and 500 °C. *Econ. Geol.*, **72**, 271–89.

Lynch, J. V. G. (1989) Large-scale hydrothermal zoning reflected in the tetrahedrite–freibergite solid solution, Keno Hill Ag–Pb–Zn district, Yukon. *Can. Mineral.*, **27**, 383–400.

Mishra, B. and Mookherjee, A. (1986) Analytical formulation of phase equilibrium in two observed sulfide–sulfosalt assemblages in the Rajpura–Dariba polymetallic deposit. *Econ. Geol.*, **81**, 627–39.

Naik, M. S. (1975) Silver sulphosalts in galena from Espeland, Norway. *Norsk Geol. Tidssk.*, **55**, 185–9.

O'Leary, M. J. and Sack, R. O. (1987) Fe–Zn exchange reaction between tetrahedrite and sphalerite in natural environments. *Contrib. Mineral. Pet.*, **96**, 415–25.

Pattrick, R. A. D. (1978) Microprobe analyses of cadmium-rich tetrahedrite from Tyndrum, Perthshire, Scotland. *Mineral. Mag.*, **42**, 286–8.

Pearson, M. F., Clark, K. F., and Porter, E. W. (1988) Mineralogy, fluid characteristics, and silver distribution at Real de Angeles, Zacatecas, Mexico. *Econ. Geol.*, **83**, 1737–59.

Ramdohr, P. (1969) *The Ore Minerals and their Intergrowths.* Pergamon, New York, 554–62.

Raabe, K. C. and Sack, R. O. (1984) Growth zoning in tetrahedrite–tennantite from the Hock Hocking mine, Alma, Colorado. *Can. Mineral.*, **22**, 577–82.

Sack, R. O. (1992) Thermochemistry of tetrahedrite–tennantite fahlores. In *The Stability of Minerals* (N. S. Ross and G. D. Price, eds.), 243–66, Chapman and Hall, London.

—— and Ghiorso, M. S. (1989) Importance of considerations of mixing properties in establishing an internally consistent thermodynamic database: thermochemistry of minerals in the system Mg_2SiO_4–Fe_2SiO_4–SiO_2. *Contrib. Mineral. Petrol.*, **102**, 41–68.

—— and Loucks, R. R. (1985) Thermodynamic properties of tetrahedrite–tennantites: Constraints on the interdependence of the Ag ⟷ Cu, Fe ⟷ Zn, Cu ⟷ Fe, and As ⟷ Sb exchange reactions. *Am. Mineral.*, **70**, 1270–89.

—— Ebel, D. S., and O'Leary, M. J. (1987) Tennahedrite thermochemistry and metal zoning. In *Chemical Transport in Metasomatic Processes* (H. C. Helgeson, ed.), 701–31. D. Reidel, Dordrecht.

Schmid, E. A., Jaffé, F. C., and Burri, M. (1990) La freibergite du gisement de plomb-zinc de Praz-Jean (Valais, Suisse). *Mineral. Deposita*, **25**, 198–204.

Springer, G. (1969) Electron probe analyses of tetrahedrite. *Neues Jahrb. Mineal. Mh.*, 24–32.

Takeuchi, Y. and Sadanago, R. (1969) Structural principles and classification of sulfosalts. *Zeit. Krist.*, **130**, 346–68.

Wu, I. and Petersen, U. (1977) Geochemistry of tetrahedrite-tennantite at Casapalca, Peru. *Econ. Geol.*, **72**, 993–1016.

Yigitgüden, H. Y. and Friedrich, G. (1986) Die Silbererzlagerstätte gümüsköy in Westanatolien, Türkei-Erzmineralparagenese und Geochemie der Silberminerale. *Erzmetall*, **39**, 14–20.

[*Manuscript received 1 August 1992: revised 10 March 1993*]